Proceeding of the 2004 American Control Conference
Boston, Massachusetts June 30 - July 2, 2004

Stability Analysis of a DiffServ Network Having Two-Level Coloring at the Network Edge and Preferential Dropping at the Core

Yong Cui, Yossi Chait and C.V. Hollot

Abstract— **This paper presents a local stability result for Differentiated Services (DiffServ) networks with heterogeneous TCP flows consisting of two-level edge coloring using a token bucket, and preferentially-dropping core router. Coloring is accomplished using a recently proposed edge mechanism to adaptively tune the token-bucket rate. The result is stated for sources under TCP-Reno congestion control algorithm. Stability analysis of several DiffServ networks that were tested using `ns` simulations is described.**

I. Introduction

The Internet was originally designed as, and by-and-large is still a framework for providing best-effort services. Traffic is processed as quickly as possible but without any guarantee of timeliness of actual delivery. In recent years, new applications have sprung which require some form of quality of service (QoS) guarantee from the network. The Internet Engineering Task Force (IETF) has proposed service models and mechanisms to meet the demand for QoS. Notably among them are the Integrated Services/Resource Reservation Protocol (RSVP) model, the Differentiated Services (DiffServ) model [13], multi-protocol label switching (MPLS) and traffic engineering. Here we focus on DiffServ which provides a scalable solution since the amount of state information is proportional to the number of contract-paying sources rather than the total number of flows. Two per-hop behaviors (PHBs) have been standardized by IETF, expedited forwarding (EF) [2] and assured forwarding (AF) [3]. The former is intended to support low delay applications while the latter is intended to provide throughput differentiation among clients according to negotiated profiles.

Our DiffServ network is based on the AF PHB. There are several traffic management and packet marking mechanisms proposed for AF DiffServ, all sharing the following basic idea. Coloring edges employ token buckets; packets that originally conform to bucket parameters (a function of a negotiated profile) are colored green and excess packets remain unmarked (colored red). Core routers give preference to green packets. In the presence of congestion, red packets are more likely to be dropped (or have their congestion notification bit set in the presence of the Explicit Congestion Notification (ECN)) [4]. Several studies have shown that the throughput attained by a customer is affected not only by the edge marker but also by the presence of other customer flows and propagation delays [5]-[7]. This is because the predominance of traffic is carried by TCP (of various variants) whose congestion avoidance mechanism reacts in a complex manner with its environment. In [8], an *Active Rate Management* (ARM) mechanism was introduced to overcome this limitation. The basic idea is that the edges maintain ARMs which are responsible for adaptively setting token bucket parameters in order to achieve minimum throughputs in the face of changing network parameters. `ns` simulations in [8] demonstrated that when combined with two-level PI AQM [9] at differentiating cores, this ARM mechanism is able to maintain minimum throughputs at or above target rates and is able to respond in a timely manner to fluctuations in traffic characteristics.

In this paper, using robust stability formulation, we analyze the effect of introducing this ARM mechanism into a stable TCP-Reno network employing PI AQM at the core. Our local stability conditions highlight the interplay between AQM and ARM and can be recast as design rules for AQM and ARM controllers. This defines the contribution of our work. The remainder of the paper is organized as follows. In Section 2 we describe a fluid model for the dynamics of the network. In Section 3 we develop linearized models for control design and analysis (details are given in /citedacs), then describe general types of AQM and ARM controllers for this problem. In Section 4, we state our main theorem that proves existence of stabilizing ARM and AQM controllers. Stability analysis of an over-provisioned and under-provisioned DiffServ networks tested in `ns` is presented in section 5. We note our parallel work in [10] which quantifies behavior of bucket-rate adaptation and preferential dropping that guarantees minimum throughput to users under general congestion control sources that include TCP-Reno and proportionally-fair schemes.

II. The DiffServ Network Model

In this section, we introduce a fluid flow model for the dynamics of a DiffServ network consisting of heterogeneous TCP-controlled sources[1], AQM-controlled core router and coloring edge routers using token buckets. Our starting

This work is supported by the National Science Foundation under Grant ANI-0125979 at the University of Massachusetts, Amherst, MA 01003.

Cui and Chait are with the MIE Department `ycui,chait@ecs.umass.edu`.
Hollot is with the ECE Department `hollot@ecs.umass.edu`.

[1]Throughout this paper the term TCP-controlled sources refers to AIMD-like sources (e.g. TCP-Reno and TCP-SACK).

point is [11] which presented a fluid flow approach for modelling TCP flows and AQM routers and the extension in [8] to account for two-color marking at the network edge and multi-level AQM at the core. The network has n classes of aggregate heterogeneous flows, termed *sources*, each consisting of η_i identical TCP flows. Without loss of generality, we assume that each such source is served by a separate edge that includes a token bucket with rate A_i and size $b_i >> 1$. The sources feed into a core router with link capacity c and queue length denoted by $q(t)$. A generic TCP flow in the i-th source is characterized by its window size $W_i(t)$ given by

$$\frac{dW_i(t)}{dt} = \frac{1-p_i(t_{\tau_i})}{\tau_i(t)} - \frac{W_i(t)W_i(t_{\tau_i})}{2\tau_i(t_{\tau_i})}p_i(t_{\tau_i}), \qquad (1)$$

where $p_i(t)$ denotes the probability that ECN bit is set for the i-th source[2] and the notation $z(t_{\tau_i}) \triangleq z(t-\tau_i)$. The average round-trip time $\tau_i(t)$ is

$$\tau_i(t) \triangleq T_{pi} + \frac{q(t)}{c}, \qquad (2)$$

where T_{pi} is the i-th source propagation delay. The source instantaneous send rate x_i is described by

$$x_i = \frac{\eta_i W_i(t)}{\tau_i(t)}. \qquad (3)$$

The dynamics of the core's buffer is described by

$$\frac{dq(t)}{dt} = -cI_{q>0} + \sum_{i=1}^{n} x_i, \qquad (4)$$

where $I_{q>0}$ is the indicator function.

Finally, we model the coloring process at an edge and multi-level AQM action at the core. To model coloring, let $f_{gi}(t)$ denote the fraction of fluid from i-th source marked green (i.e., flow within target rate) where

$$f_{gi}(t) = \min\left\{1, \frac{A_i(t)}{x_i(t)}\right\},$$

and $1 - f_{gi}(t)$ denotes the red fraction of flow (exceeding target rate). At the core, $p_g(t)$ and $p_r(t)$ denote the probabilities that ECN marks are generated for the green and red fluids, respectively[3]. According to [15], we have $0 \le p_g(t) < p_r(t) \le 1$. The i-th source's loss probability $p_i(t)$ is then related to the green and red marks by

$$p_i(t) = f_{gi}(t)p_g(t) + (1 - f_{gi}(t))p_r(t). \qquad (5)$$

Next, in preparation for stability analysis of the network, we derive a linearized model about equilibrium.

[2]The $1 - p_i$ term in the additive part does not appear in [8], but has appeared since in several publications, e.g., [12].

[3]More precisely, marks are embedded in the fluid as a time varying Poisson process, and the product of p_g and p_r with the green and red fluid throughputs, respectively, determines the intensity of this Poisson process.

III. Linearized Network Model

In this section, we linearize the network model (1)-(5) about equilibrium, then form control block diagram suited for stability analysis. We follow with the token bucket controllers and AQMs which complete description of the closed-loop system.

A. Open-Loop Model

We begin by writing the model explicitly in terms of the bucket rates A_i:

$$\begin{aligned}
\dot{q} &= -cI_{q>0} + \sum_{i=1}^{n} \frac{\eta_i W_i(t)}{\tau_i} \\
&\triangleq f(q, W_i, p_g, p_r, A_i); \\
\dot{W}_i &= \frac{1-p_i(t_{\tau_i})}{\tau_i(t)} - \frac{W_i(t)W_i(t_{\tau_i})}{2\tau_i(t_{\tau_i})}p_i(t_{\tau_i}) \\
&\triangleq g_i(q, W_i, p_g, p_r, A_i)
\end{aligned}$$

where

$$p_i = \left(\frac{A_i}{x_i}p_g + (1 - \frac{A_i}{x_i})p_r\right).$$

Let the equilibrium state be denoted by $(\hat{q}, \hat{W}_i, \hat{p_g}, \hat{p_r}, \hat{A}_i)$ and denote perturbations about equilibrium by $\delta z \triangleq z(t) - \hat{z}$. The linearized open-loop network model can be shown to be (see [17] for details)

$$\begin{aligned}
\delta W_i(s) &= \frac{\frac{\partial g_i}{\partial A_i}}{s - \frac{\partial g_i}{\partial W_i}}\delta A_i(s) + \frac{\frac{\partial g_i}{\partial p_g}}{s - \frac{\partial g_i}{\partial W_i}}e^{-s\tau_i}\delta p_g(s) \\
&\quad + \frac{\frac{\partial g_i}{\partial p_r}}{s - \frac{\partial g_i}{\partial W_i}}e^{-s\tau_i}\delta p_r(s) \qquad (6) \\
\delta q(s) &= \sum_{i=1}^{n} \frac{\frac{\partial f}{\partial W_i}}{s - \frac{\partial f}{\partial q}}\delta W_i(s).
\end{aligned}$$

In [17] it is shown that at equilibrium, either $\delta p_r(s)$ or $\delta p_g(s)$ are fixed. The choice of $\delta p_r(s)$ above corresponds to an over-provisioned network. Similar relations can be derived in the under-provisioned case in terms of $p_g(s)$.

B. Network Controllers

In [9], a PI-type AQM was proposed as a congestion controller at core routers. This AQM was shown to be able to maintain buffer level at reference set point in the face of dynamic network conditions. Token buckets were introduced in order to maintain source throughput at a target rate $\underline{x}$. However, [11] showed that one cannot guarantee that resulting throughputs are equal to or greater than the bucket rate. To overcome this inherent limitation, [8] proposed a feedback structure around a token bucket termed ARM. The purpose of ARM is to regulate the token bucket rate A_i such that $x_i \ge \underline{x}_i$ (if the network is sufficiently provisioned). Indeed, following the ideas behind the PI AQM, the ARM controller has the structure

$$ARM(s) = \frac{k_{arm}(\frac{s}{z_{arm}} + 1)}{s(\frac{s}{p_{arm}} + 1)}.$$

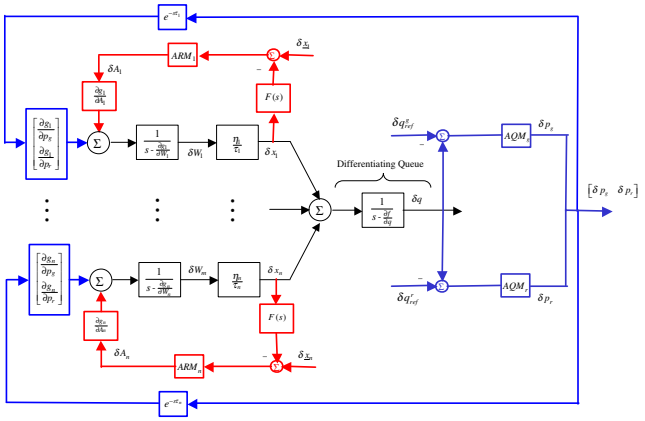

Fig. 1. The combined ARM/AQM DiffServ network.

Note that ARM compares source rate to its bucket rate, hence, it is necessary to construct rate estimation. This is done using a modified TSW (Time-Slice Window) procedure [14]: the source rate estimate is computed by measuring the number of sent packets over a fixed time period T_{TSW} and further smoothed by a low-pass filter F. The transfer function representing this estimation is given by

$$F(s) = \frac{a}{s+a} e^{-sT_{TSW}}.$$

DiffServ stipulates that AQMs differentiate between green packets (those within their target rates) and red packets. The idea is to give preference to packets corresponding to sources within their target rates. We accomplish this using a multi-level PI AQM, one for green flow and a second for the red flow, along with set points, q^g_{ref} and q^r_{ref}, respectively. The marking probabilities, p_g and p_r, for the green and red fluid, respectively, are computed by the two PI AQM controllers, $AQM_g(s)$ and $AQM_r(s)$. Setting $q^g_{ref} > q^r_{ref}$ insures that red packets are marked before green packets [10]. We use the same controller in both loops, that is,

$$AQM(s) = AQM_g(s) = AQM_r(s) = \frac{k_{aqm}(\frac{s}{z_{aqm}} + 1)}{s}.$$

Combining the open-loop network model with the ARM and AQM controllers leads to the closed-loop block diagram of the DiffServ network shown in Figure 1. Next, we analyze local stability of this network.

IV. Stability of DiffServ Networks

In this section, we discuss the effect of ARM on stability of the DiffServ network. The network's linearized model, shown in Figure 1, comprises of n heterogeneous TCP sources with n ARM loops. We now present our main result.

Theorem: *Consider the linearized DiffServ network shown in Figure 1. There exist AQM and $\{ARM_j : j = 1, \ldots, n\}$ such that the system is locally stable.*

Proof. We start with a sketch of the proof. The block diagram in Figure 1 is redrawn in Figure 2 to show a

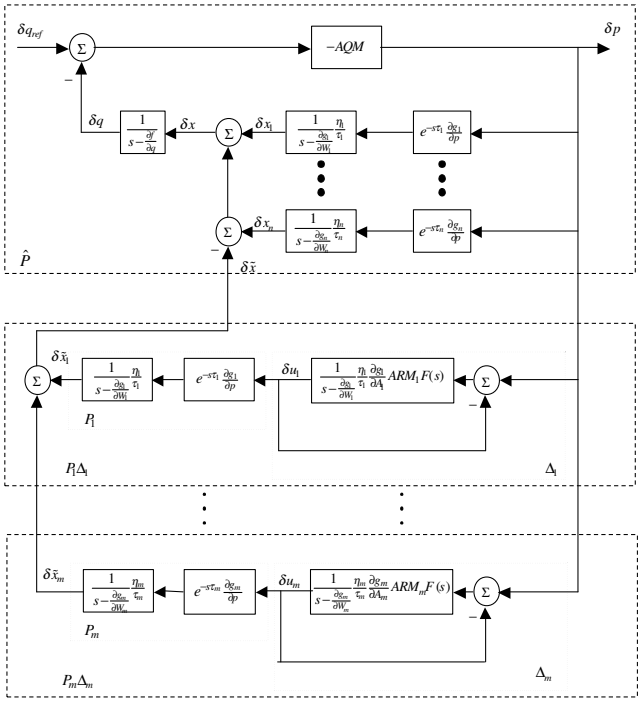

Fig. 2. Block diagram of AQM networks with active ARM loops (the perturbation blocks indexes correspond to those in the set J).

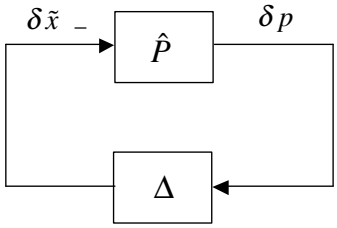

Fig. 3. Simplified block diagram of the system in Figure 2.

nominal (i.e., without ARMs) TCP/AQM network along with perturbations due to active ARMs. A network we comprises of n heterogeneous TCP sources with m active ARM loops (see [17]), where $m < n$ (see [15]). The set of active ARM loops is defined by $J \triangleq \{1 \leq j \leq n : \ j^{th}$ ARM loop is active at equilibrium$\}$. That is, if $ARM_i = 0, i = 1, \ldots, n$, then the block diagram reduces to a series connection between the open-loop network in Figure 7 and the AQM (albeit single controller). These perturbations can be combined into a single block as shown in Figure 3. We then apply small gain arguments to establish closed-loop stability.

The nominal TCP/AQM system in Figure 2, denoted by $\hat{P}$, is described by

$$\begin{aligned} \hat{P}(s) \ &\triangleq \ \frac{\delta p}{\delta \hat{x}} = \frac{\frac{1}{s - \frac{\partial f}{\partial q}} AQM}{1 - \frac{1}{s - \frac{\partial f}{\partial q}} AQM \sum_{i=1}^{n} P_i} \\ &\triangleq \ \frac{\frac{1}{s - \frac{\partial f}{\partial q}} AQM}{1 - L(s)}, \end{aligned} \tag{7}$$

where $\delta\tilde{x}$ is the total rate perturbation from nominal TCP/AQM value due to active ARMs: $\delta\hat{x} = \sum_{i\in J}\delta\hat{x}_i$ and $\delta\hat{x}_i = P_i\Delta_i\delta p$. The source's TCP transfer function P_i is given by

$$P_i = e^{-s\tau_i}\frac{\partial g_i}{\partial p}\frac{1}{s-\frac{\partial g_i}{\partial W_i}}\frac{\eta_i}{\tau_i},$$

with ARM-induced perturbation $\Delta_j(s)$:

$$\Delta_j(s) = \frac{\frac{1}{s-\frac{\partial g_j}{\partial W_j}}\frac{\eta_j}{\tau_j}\frac{\partial g_j}{\partial A_j}ARM_j\cdot F_j(s)}{1+\frac{1}{s-\frac{\partial g_j}{\partial W_j}}\frac{\eta_j}{\tau_j}\frac{\partial g_j}{\partial A_j}ARM_j\cdot F_j(s)}.$$

Note that due to the Δ_i block, the marking probability δu_i experienced by a source with an active ARM is different from the AQM's δp. Finally, a simplified formulation of this system with a single perturbation block Δ is shown in Figure 3 where $\Delta(s) = \sum_{j\in J}P_j\Delta_j(s)$.

Next, we derive upper bounds on the AQM and ARM gains guaranteeing stability of $\hat{P}$ and Δ, then provide additional bounds on these gains such that $\|\hat{P}\Delta\|_\infty < 1$. These gain constraints are used to show that the system in Figure 3 is stable which implies stability of the system in Figure 1.

To analyze stability of Δ it is sufficient to discuss stability of Δ_j as follows. We use Nyquist stability criteria to show that there exists $k_{arm_j} > 0$ stabilizing Δ_j. Δ_j can be written as this closed-loop system

$$\Delta_j(s) = \frac{L_{\Delta_j}(s)}{1+L_{\Delta_j}(s)}$$

where $L_{\Delta_j}(s)$ is given by

$$L_{\Delta_j}(s) = \frac{1}{s-\frac{\partial g_j}{\partial W_j}}\frac{\eta_j}{\tau_j}\frac{\partial g_j}{\partial A_j}ARM_jF_j(s). \tag{8}$$

Since $L_{\Delta_j}(s)$ has a pole at the origin, it is necessary that the Nyquist contour Γ includes an infinitesimal semicircle Γ_ϵ around $s=0$ described by

$$\Gamma_\epsilon \triangleq \{s = \epsilon e^{j\theta};\ \ \theta\in[-90^\circ, 90^\circ],\ \epsilon\to 0,\ \epsilon>0\} \tag{9}$$

As s traverses from $-j\epsilon$ to $+j\epsilon$ along Γ_ϵ, θ changes from -90° to $+90^\circ$ counterclockwise. The corresponding Nyquist plot of $L_{\Delta_j}(s)$ can be determined by evaluating (8) along (9). In the limit we have,

$$\lim_{\epsilon\to 0}L_{\Delta_j}(\epsilon e^{j\theta}) = \frac{1}{-\frac{\partial g_j}{\partial W_j}}\frac{\eta_j}{\tau_j}\frac{\partial g_j}{\partial A_j}\frac{k_{arm_j}}{\epsilon e^{j\theta}}.$$

It is seen that any instabilities in $\Delta_j(s)$ will be a result of encirclements by the Nyquist plot of $L_{\Delta_j}(s)$ over the range $\omega\in(\epsilon,+\infty)\cup(-\epsilon,-\infty)$. Define $L_{\Delta_j}(j\omega) = k_{arm_j}\tilde{L}_{\Delta_j}(j\omega)$. The plot of $\tilde{L}_{\Delta_j}(j\omega)$ crosses the negative real-axis at frequencies in the set $\Omega = \{\omega : \angle\tilde{L}_{\Delta_j}(j\omega) = -180^\circ\}$. Let ω_1 be the frequency such that $|\tilde{L}_{\Delta_j}(j\omega_1)| = \max_{\omega\in\Omega}|\tilde{L}_{\Delta_j}(j\omega)|$. If $k_{arm_j} < |\tilde{L}_{\Delta_j}(j\omega_1)|^{-1}$ then $|L_{\Delta_j}(j\omega)| < 1$ implying stability of Δ_j. Stability of Δ follows immediately from $k_{arm_j} < |\tilde{L}_{\Delta_j}(j\omega_1)|^{-1},\ \ j=1,\ldots,n$.

Next, we show that $|\hat{P}(j\omega)\Delta(j\omega)| < 1$ over the ranges $[0,\omega_0]$ and $[\omega_0,\infty]$, where ω_0 is a sufficiently small frequency to be defined later. To this end, we now show that $\|\Delta_j(s)\|_\infty = 1$ which is used later. Let $Re(L_{\Delta_j}(j\omega))$ denote the real part of $L_{\Delta_j}(j\omega)$ and let ω_2 be the frequency where $Re(\tilde{L}_{\Delta_j}(j\omega_2)) = \min_{\omega\in\Gamma}Re(\tilde{L}_{\Delta_j}(j\omega))$. Hence, $Re(L_{\Delta_j}(j\omega)) > -\frac{1}{2}$ if $k_{arm_j} < 2|Re(\tilde{L}_{\Delta_j}(j\omega_2))|^{-1}$, or equivalently $\left|\frac{L_{\Delta_j}(j\omega)}{1+L_{\Delta_j}(j\omega)}\right| < 1$ [16]. Noting that $|\Delta_j(j\omega)| = 1$ at $\omega=0$ (due to the integrator), we have shown that to have $\|\Delta_j(j\omega)\|_\infty = 1$ we need

$$k_{arm_j} < \min\left\{\frac{1}{2|Re(\tilde{L}_{\Delta_j}(j\omega_2)|}, \frac{1}{|\tilde{L}_{\Delta_j}(j\omega_1)|}\right\}. \tag{10}$$

Now consider the product $|\hat{P}(j\omega)\Delta(j\omega)|$ over the range $\omega\in[0,\omega_0]$. First, we can bound Δ as by

$$|\Delta(j\omega)| \leqslant \sum_{j\in J}|P_j(j\omega)|. \tag{11}$$

Rewrite $\hat{P}$ in terms of $\sum_{j\in J}|P_j(j\omega)|$

$$\hat{P} = \left|\frac{\frac{1}{j\omega-\frac{\partial f}{\partial q}}AQM(\sum_{i=1}^n P_i(j\omega))}{1-\frac{1}{j\omega-\frac{\partial f}{\partial q}}AQM(\sum_{i=1}^n P_i(j\omega))}\right|\left|\frac{1}{\sum_{i=1}^n P_i(j\omega)}\right|$$

and show that

$$\left\|\frac{\frac{1}{j\omega-\frac{\partial f}{\partial q}}AQM(\sum_{i=1}^n P_i(j\omega))}{1-\frac{1}{j\omega-\frac{\partial f}{\partial q}}AQM(\sum_{i=1}^n P_i(j\omega))}\right\|_\infty \triangleq \left\|\frac{L_{\hat{P}}(j\omega)}{1+L_{\hat{P}}(j\omega)}\right\|_\infty$$

equals unity. At $\omega=0$, due to the AQM's integrator

$$\left|\frac{\frac{1}{j\omega-\frac{\partial f}{\partial q}}AQM(\sum_{i=1}^n P_i(j\omega))}{1-\frac{1}{j\omega-\frac{\partial f}{\partial q}}AQM(\sum_{i=1}^n P_i(j\omega))}\right| = 1.$$

Let $Re(L_{\hat{P}}(j\omega))$ denote the real part of $L_{\hat{P}}(j\omega)$ with the factorization $Re(L_{\hat{P}}(j\omega)) = k_{aqm}Re(\tilde{L}_{\hat{P}}(j\omega))$. Let ω_3 be the frequency where $Re(\tilde{L}_{\hat{P}}(j\omega_3)) = \min_{\omega\in\Gamma}Re(\tilde{L}_{\hat{P}}(j\omega))$. Hence, $Re(L_{\hat{P}}(j\omega)) > -\frac{1}{2}$ if $k_{aqm} < 2|Re(\tilde{L}_{\hat{P}}(j\omega_3))|^{-1}$, or equivalently, $\left|\frac{L_{\hat{P}}(j\omega)}{1+L_{\hat{P}}(j\omega)}\right| < 1$ [16]. This proves that if $k_{aqm} < \frac{1}{2|Re(\tilde{L}_{\hat{P}}(j\omega_3))|}$ then

$$\left\|\frac{\frac{1}{j\omega-\frac{\partial f}{\partial q}}AQM(\sum_{i=1}^n P_i(j\omega))}{1-\frac{1}{j\omega-\frac{\partial f}{\partial q}}AQM(\sum_{i=1}^n P_i(j\omega))}\right\|_\infty = 1. \tag{12}$$

It follows from (12) that

$$|\hat{P}(j\omega)| \leq \left|\frac{1}{\sum_{i=1}^n P_i(j\omega)}\right|. \tag{13}$$

Combining (11)-(13) we obtain

$$|\hat{P}(j\omega)\Delta(j\omega)| \leqslant \frac{\sum_{j\in J}|P_j(j\omega)|}{|\sum_{i=1}^n P_i(j\omega)|}.$$

We observe that the right-hand side of the above) is a continuous function of ω, and at $\omega = 0$ it is smaller than 1. Thus, given any $0 < \epsilon_1 \ll 1$, there exists a sufficiently small frequency ω_0, such that

$$\left| \frac{\sum_{j\in J} |P_j(j\omega)|}{|\sum_{i=1}^n P_i(j\omega)|} - \frac{\sum_{j\in J} |P_j(j0)|}{|\sum_{i=1}^n P_i(j0)|} \right| \leq \epsilon_1, \ |\omega - 0| \leq \omega_0.$$

Hence

$$\left| \frac{\sum_{j\in J} |P_j(j\omega)|}{|\sum_{i=1}^n P_i(j\omega)|} \right| < 1, \ \forall \omega \in [0, \omega_0].$$

and we proved that if k_{aqm} stabilizes $\hat{P}$ (see [17]) and satisfies (12), then $|\hat{P}(j\omega)\Delta(j\omega)| < 1, \ \forall \omega \in [0, \omega_0]$.

Finally, we show that $|\hat{P}(j\omega)\Delta(j\omega)| < 1$ over $\omega \in [\omega_0, \infty)$. $|L(j\omega)|$ in (7) can be expanded as follows

$$\begin{aligned} |L(j\omega)| \ &\leq \ \left| \frac{1}{j\omega - \frac{\partial f}{\partial q}} \right| \left| \frac{k_{aqm}(\frac{j\omega}{z_{aqm}} + 1)}{j\omega} \right| \sum_{i=1}^n \left| e^{-j\omega\tau_i} \right| \\ &\quad \times \left| \frac{\partial g_i}{\partial p} \right| \left| \frac{1}{j\omega - \frac{\partial g_i}{\partial W_i}} \right| \left| \frac{\eta_i}{\tau_i} \right|. \end{aligned}$$

At $\omega \geq \omega_0$, we can show that

$$\begin{aligned} |L(j\omega)| \ &< \ \left| \frac{1}{\omega_0} \right| \left| k_{aqm} \sqrt{\left(\frac{1}{z_{aqm}}\right)^2 + \left(\frac{1}{\omega_0}\right)^2} \right| \\ &\quad \times \sum_{i=1}^n \left| \frac{\partial g_i}{\partial p} \right| \left| \frac{1}{\omega_0} \right| \left| \frac{\eta_i}{\tau_i} \right| \\ &\triangleq \ M k_{aqm} < \infty. \end{aligned}$$

Hence, $k_{aqm} < \frac{\epsilon_2}{M} \Longrightarrow |L(j\omega)| < \epsilon_2, \ \omega \in [\omega_0, \infty)$. From the above

$$|\hat{P}(j\omega)| < \left| \frac{\frac{1}{j\omega - \frac{\partial f}{\partial q}} \frac{k_{aqm}(\frac{j\omega}{z_{aqm}} + 1)}{j\omega}}{1 - \epsilon_2} \right|.$$

To bound $|\hat{P}|$ consider the product $m \left| \frac{k_{max}}{j\omega + p_{min}} \right| |\hat{P}(j\omega)|$ which can be shown to be bounded by

$$\begin{aligned} &(n-1) \left| \frac{k_{max}}{\omega_0^2} \right| \left| \frac{1}{1 - \epsilon_2} \right| \left| k_{aqm} \sqrt{\left(\frac{1}{z_{aqm}}\right)^2 + \left(-\frac{1}{\omega_0}\right)^2} \right| \\ &\triangleq \tilde{M} k_{aqm} < \infty, \end{aligned}$$

where $k_{max} \triangleq \max_{j\in J} \left\{ \left| \frac{\partial g_j}{\partial p} \frac{\eta_j}{\tau_j} \right| \right\}$ and $p_{min} \triangleq \min_{j\in J} \left\{ -\frac{\partial g_j}{\partial W_j} \right\}$. Since The term $|\Delta|$ over $\omega \in [\omega_0, \infty)$ can be bounded as follows

$$|\Delta| \leq (n-1) \left| \frac{k_{max}}{j\omega + p_{min}} \right|,$$

then we have shown that over the range $\omega \in [\omega_0, \infty)$, if $k_{aqm} < \min \left\{ \frac{\epsilon_1}{M}, \frac{1}{\tilde{M}} \right\}$ then $|\hat{P}(j\omega)| < \left| m \frac{k_{max}}{j\omega + p_{min}} \right|^{-1}$. The term $|\Delta|$ can be bounded as follows

$$|\Delta| \leq (n-1) \left| \frac{k_{max}}{j\omega + p_{min}} \right|, \ \omega \in [\omega_0, \infty).$$

Hence, if $k_{aqm} < \min \left\{ \frac{\epsilon_1}{M}, \frac{1}{\tilde{M}} \right\}$ then $|\hat{P}(j\omega)\Delta(j\omega)| < 1, \ \forall \omega \in [\omega_0, \infty)$. Finally, if the ARMs gains are bounded by (10) for $j = 1, \ldots, n$, then

$$k_{arm_j} < \min \left\{ \frac{1}{2|Re(\tilde{L}_{\Delta_j}(j\omega_2)|}, \frac{1}{|\tilde{L}_{\Delta_j}(j\omega_1)|} \right\},$$

and the AQM gains are bounded by

$$k_{aqm} < \min \left\{ \frac{1}{2|Re(\tilde{L}_{\hat{P}}(j\omega_3))|}, \frac{\epsilon_1}{M}, \frac{1}{\tilde{M}}, \frac{1}{|\tilde{L}(j\omega_4)|} \right\}$$

then both $\hat{P}$ and Δ are stable and $\|\hat{P}(j\omega)\Delta(j\omega)\|_\infty = 1$. Hence, we have shown that the DiffServ network shown in Figure 1 is locally stable if k_{aqm} and k_{arm} satisfy their gain constraints. This proves that there exist AQM and $\{ARM_j : \ j = 1, \ldots, n\}$ such that the system is locally stable. □

V. Illustrative Examples

In this section, we apply the Theorem to analyze stability of the DiffServ network in [8]. This network consisted of three heterogeneous sources, each served by an edge with fully-coloring ARM as shown in Figure (4). The edges feed into a congested core with an admissible, compatible and non-overlapping differentiation ability (see [17] and [10]). The propagation delays T_{pi} are all uniform in the ranges: $T_{p1} \in [50 - 90]$ msec, $T_{p2} \in [15 - 25]$ msec and $T_{p3} \in [0 - 10]$ milliseconds. Each source is an aggregate of η_i generic FTP flows, all starting uniformly in $[0, 50]$ sec, with loads $\eta_1 = 20$, $\eta_2 = 30$ and $\eta_3 = 25$. The core queue has a buffer size of 800 packets and ECN marking enabled. The source target rates are $\underline{x}_1 = 2000$, $\underline{x}_2 = 500$ and $\underline{x}_3 = 1250$ packet/second.

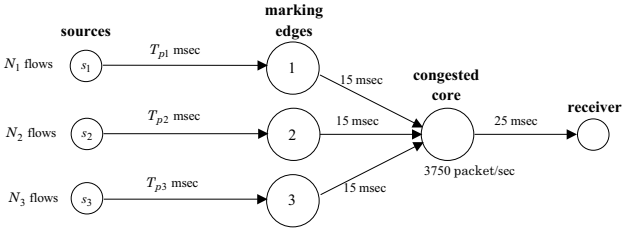

Fig. 4. The simulated DiffServ network.

The same AQM controller was used for green and red flows and is given by $AQM(s) = 9.6 \times 10^{-6}(\frac{s}{0.53} + 1)s^{-1}$. The set points for the red and green controllers were $q^r_{ref} = 100$ packets and $q^g_{ref} = 250$ packets. The idea behind this choice is while fully utilizing the link also minimize the possibility of the queue oscillating between these points due to incoming flow bursts.

In [8], the ARMs are the same where $ARM_j(s) = \frac{0.05(\frac{s}{0.1}+1)}{s(s+1)}; \ j = 1, 2, 3$. The source rate estimator implements the modified TSW algorithm with the three buckets using $T_{TSW} = 1$ second. It is further smoothed by a first-order, low-pass filter with a corner frequency of $a = 1$

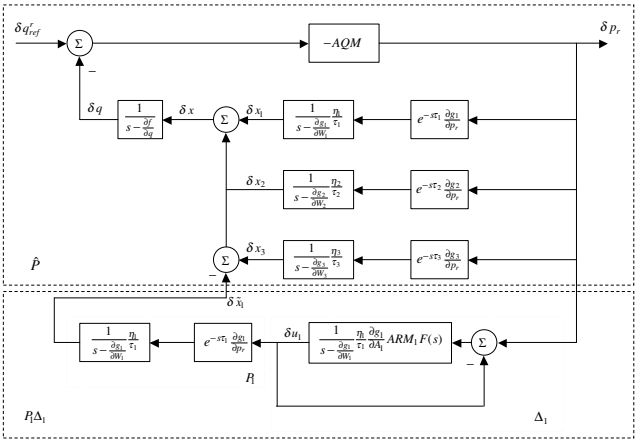

Fig. 5. Block diagram of the over-provisioned network (see [17] for a full-size figure of this and other figures in this paper).

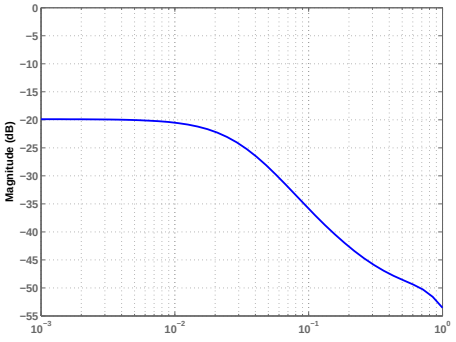

Fig. 6. The magnitude Bode plot of $\hat{P}\Delta$ (over-provisioned case).

rad/second with the transfer function $F(s)$ of $F(s) = \frac{1}{s+1}e^{-s}$. We analyze stability of two implementations, an over-provisioned and an under-provisioned network.

A. Over-Provisioned Network

In the over-provisioned case, the link capacity is $c = 4500$ packets/second. In [17] it is shown that the queue length at equilibrium is at $q^r_{ref} = 100$ packets with $p_r < 1$, $p_g = 0$. Hence, the round trip times are $\tau_1 = 0.24$ second, $\tau_2 = 0.14$ second and $\tau_3 = 0.11$ second. According to [15], $\frac{x_1}{\alpha_1} > \frac{x_3}{\alpha_3} > \frac{x_2}{\alpha_2}$, where $\alpha_i = \frac{\eta_i}{\tau_i}$. We also compute $i^* = 2$ (see [15]) implying that the second and the third ARMs are de-activated and $J = \{1\}$. The generalized system block diagram in Figure 2 can be reduced in this case to the one shown in Figure 5 where the nominal TCP/AQM system is described by (7) where $i = 3$. Numerical values of this feedback system can be found in [17]. We observe in Figure 6 that $\|\hat{P}\Delta\|_\infty < 1$, which along with stability of $\hat{P}$ and Δ (not shown here) establishes local stability of this DiffServ network. Further details and simulation plots can be found in [10].

B. Under-Provisioned Network

In this setup, the link capacity is 20% under provisioned where $c = 3000$ packets/second. From [17], it follows that $p_r = 1, 0 < p_g < 1$,and $q = q^g_{ref} = 250$ packets. Stability analysis, similar to that done above is given in [17].

VI. Conclusions

We analyzed stability of DiffServ networks with heterogeneous TCP flows consisting of two-level edge coloring using a token bucket, and preferentially-dropping core router. We have shown, in terms of gain bounds, the existence of stabilizing AQM and ARM controllers. This stability result complements our earlier work in [8] which described ns implementations and current work in [10] which quantified behavior of bucket-rate adaptation and preferential dropping that guarantees minimum throughput to users under general congestion control sources. We are presently working on generalization of this DiffServ architecture to networks with multiple congested cores.

References

[1] S. Blake, D. Black, M. Carlson, E. Davies, Z. Wang, and W. Weiss, "An architecture for Differentiated Services," *RFC2475*, Network Working Group, Dec. 1998.

[2] V. Jacobson, K. Nichols, and K. Poduri, "An expedited forwarding PHB," *RFC2598*, 1999.

[3] J. Heinanen, F. Baker, W. Weiss, and J. Wroclawski, "Assured forwarding goup," *RFC2597*, 1999.

[4] K.K. Ramakrishnan, and S. Floyd, "Proposal To Add Explicit Congestion Notification (ECN) to IP," *RFC 2481*, 1999.

[5] S. Sahu, P. Nain, D. Towsley, C. Diot, and V. Firoiu, "On Achievable Service Differentiation with Token Bucket Marking for TCP," *Procs. ACM SIGMETRICS*, pg. 23-33, 2000.

[6] I. Yeom, and A. L. N. Reddy, "Modeling TCP behavior in a Differentiated-Services Network," *ACM/IEEE Trans. Networking*, 2001.

[7] M. Goyal, A. Durresi, P. Misra, C. Liu, R. Jain, "Effect of Number of Drop Precedences in Assured Forwarding," *Procs. GlobeCom*, 1999.

[8] Y. Chait, C.V. Hollot, V. Misra, D. Towsley, H. Zhang,and C.S. Lui, "Throughput Guarantees for TCP Flows Using Adaptive Two Color Marking and Multi-Level AQM," *Procs. INFOCOM*, pg. 837-844, 2002.

[9] C. V. Hollot, V. Misra, D. Towsley, and W. B. Gong, "On designing improved controllers for aqm routers supporting tcp flows," in *Procs. INFOCOM*, 2001.

[10] Y. Chait, C.V. Hollot, V. Misra, D. Towsley, H. Zhang, C.S. Lui, and Y. Cui "Guaranteed Throughput Using Adaptive Two-Level Coloring at the Network Edge and Preferential Dropping at the Core," *ACM/IEEE Trans. Networking*, submitted; available upon request.

[11] V. Misra, W. Gong, and D. Towsley. "Fluid-based analysis of a network of AQM routers supporting TCP flows with an application to RED," *Procs. ACM SIGCOMM*, 2000.

[12] S. H. Low, F. Paganini, and J. C. Doyle, "Internet Congestion Control," *IEEE Control Systems Magazine*, 22(1), pg. 28-43, 2002.

[13] S. Blake, D. Black, M. Carlson, E. Davies, Z. Wang, and W. Weiss, "An architecture for Differentiated Services," *RFC2475*, Network Working Group, Dec. 1998.

[14] D. D. Clark, and W. Fang, "Explicit allocation of best effort packet delivery service." *IEEE/ACM Transactions on Networking*, 1998.

[15] Y. Chait, and C.V. Hollot,"Fixed Point of a TCP/RENO DiffServ Network with a Single Congested Link ," DACS Lab, *Technical Report DACS02-07*, 2003.

[16] K. Ogata, *Modern Control Engineering*, 4th Edition, Prentice Hall, NJ. 2002.

[17] http://www.ecs.umass.edu/mie/labs/dacs/.